Advanced Synthesis & Catalysis

ADVANCED SYNTHESIS & CATALYSIS
advsynthcatal.com

RESEARCH ARTICLE OPEN ACCESS

Rhodium Multitasking Catalysis Integrating Long-Range Isomerization, Cycloisomerization, and Hydrosilylation of 1,n-Dienes to Give 2,3-Disubstituted Dihydrobenzofurans: Mechanistic Insight Into Functionalization-Controlled Reactivity

Masaharu Takatsuki[1] | Yuta Sato[1] | Tsuyoshi Matsuzaki[2] | Makoto Sako[1] | Atsushi Nakayama[1] | Takeyuki Suzuki[2] | Mitsuhiro Arisawa[1]

[1]Graduate School of Pharmaceutical Sciences, The University of Osaka, Osaka, Japan | [2]Comprehensive Analysis Center, SANKEN, The University of Osaka, Osaka, Japan

Correspondence: Mitsuhiro Arisawa (arisaw@phs.osaka-u.ac.jp)

Received: 12 October 2025 | **Revised:** 25 November 2025 | **Accepted:** 27 November 2025

Keywords: cycloisomerization | hydrosilylation | long-range isomerization | multitask catalyst | rhodium catalyst

ABSTRACT

Multitasking catalysis offers a robust and sustainable strategy for achieving multiple transformations within a single catalytic system. Herein, we describe a rhodium-catalyzed multitasking sequence that orchestrates long-range isomerization, cycloisomerization, and hydrosilylation of 1,n-dienes in a single operation. This work represents the first demonstration of a single catalytic system capable of performing these three distinct reactions consecutively. The transformation efficiently delivers silylated 2,3-disubstituted dihydrobenzofuran derivatives, which are key structural motifs in bioactive and functional molecules. Systematic optimization revealed that the hydrosilylation step is highly sensitive to the steric and electronic properties of the silane reagent. Mechanistic investigations, including in situ ^{1}H NMR analyses, indicated that the hydrosilane strongly influences the equilibrium of long-range isomerization by modulating the availability of catalytically active Rh–H species. In contrast to our previously developed hydroboration system, the current hydrosilylation conditions suppress alkene migration, resulting in limited product convergence. These findings uncover how the terminal functionalization reagent governs multitasking catalysis and provide valuable insight for designing next-generation integrated catalytic systems.

1 | Introduction

Heterocycles constitute central structural units that govern molecular function in pharmaceuticals, bioactive compounds, functional molecules, and numerous natural products [1–3]. In such compounds, ring systems incorporating heteroatoms such as oxygen and nitrogen regulate molecular conformation and electronic properties, thereby making significant contributions to biological activities and physicochemical behavior. Among them, the benzofuran framework, which contains an oxygen atom within the ring, is recognized as necessary in both medicinal and materials chemistry, and efficient methods for constructing polysubstituted benzofurans have been investigated for decades [4–7]. However, access to these scaffolds generally requires multistep sequences with intervening purifications, leading to high environmental burdens associated with step count and solvent usage.

A multitasking catalysis [8–13], in which a single catalytic system that can promote several distinct chemical transformations, has

emerged as a promising strategy in sustainable organic synthesis. By integrating several reaction steps under a unified catalytic environment, this approach reduces waste, shortens synthetic routes, and enables efficient construction of complex molecular architectures (Figure 1a) [14–20]. A variety of multitasking catalytic systems have been developed, including those capable of performing oxidation–reduction, hydrofunctionalization, and C—C bond-forming sequences [21, 22]. Despite these advances, systems that accomplish three or more distinct transformations with a single catalyst have emerged as a new concept aligned with the goals of sustainable synthesis.

In this research background, we recently reported a rhodium-based multitasking catalysis that affects three reactions, long-range isomerization/cycloisomerization/hydroboration of 1,n-dienes (Figure 1b) [23]. In that process, sequential isomerization of the diene relocates the alkene to a suitable position to trigger cyclization, followed by hydroboration to furnish 2,3-disubstituted dihydrobenzofuran derivatives in high yields. This outcome constitutes a vital demonstration that multitasking catalysts can integratively control three reactions to give polysubstituted heterocycles.

Building on this foundation, we sought to gain new mechanistic insight into this rhodium multitasking system by replacing the terminal hydroboration step with a different functionalization —hydrosilylation (Figure 1c).

We found that, after long-range isomerization and cycloisomerization of 1,n-dienes to form intermediate **II** bearing a dihydrobenzofuran framework, the terminal alkene of intermediate **II** undergoes consecutive hydrosilylation to give silylated 2,3-disubstituted dihydrobenzofurans. To the best of our knowledge, there are no previous examples in which a single catalytic system accomplishes sequential long-range isomerization, cycloisomerization, and hydrosilylation.

The present study thus not only establishes the first rhodium multitasking catalyst capable of executing these transformations but also reveals that the nature of the hydrosilylation reagent profoundly influences the alkene-isomerization equilibrium, thereby providing new mechanistic insight into multitasking catalysis.

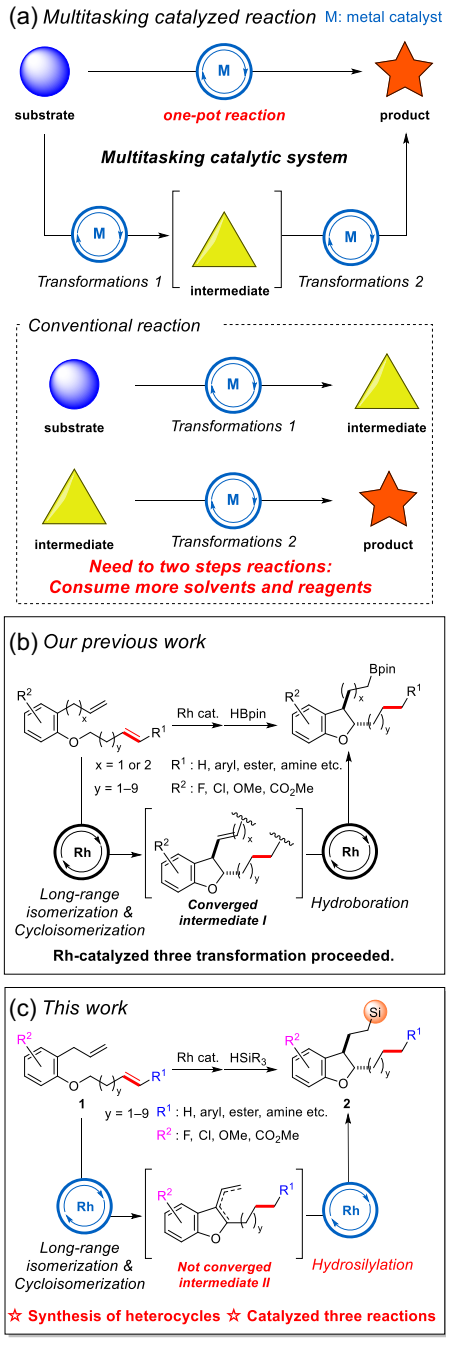

FIGURE 1 | Multitasking catalyzed reactions. (a) Multitasking catalyzed reaction. (b) Our previous work. (c) This work.

2 | Result and Discussion

2.1 | Reaction Optimization

We previously reported a one-pot long-range isomerization/cycloisomerization/hydroboration of alkenes using a rhodium catalyst [23]. In the present work, we optimized the reaction conditions to obtain hydrosilylated dihydrobenzofuran **2** from the terminal-alkene substrate **1a** (Table 1).

In entry 1, we began from the optimal conditions established in our earlier work [23]. A *p*-xylene solution of substrate **1a** (0.100 mmol), $[Rh(CH_2{=}CH_2)Cl]_2$ (10 mol%), tris-2,4,6-trimethylphosphine (30 mol%), and AgOTf (10 mol%) was stirred at 110°C for 14 h. After cooling to 60°C, triethylsilane (3.0 equiv.) was added and the mixture was stirred for an additional 2 h. Product **2a** bearing a silyl group was obtained in 88% NMR yield and 86% isolated yield. (In this study, we examined the reaction using the chiral ligands (L1–L5) shown below; however, no cyclized products were obtained. Further investigations to address this issue are currently underway).

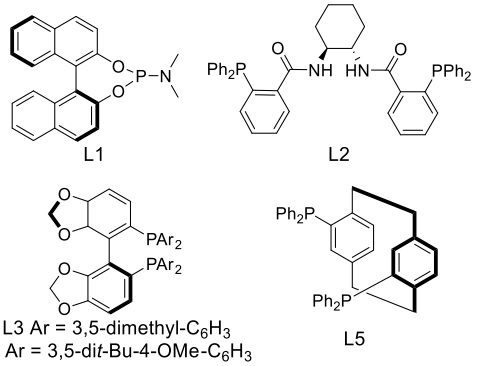

In entry 2, guided by precedents in rhodium-based multitasking catalysis [20], we removed the phosphine ligand and examined Wilkinson's catalyst under otherwise identical conditions; no

TABLE 1 | Optimization of reaction conditions.

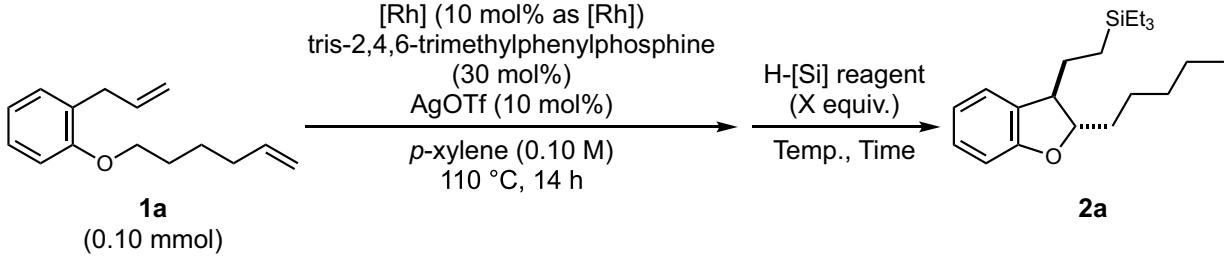

1a
(0.10 mmol)

2a

Entry	[Rh]	H-[Si]reagent	X	Temp., °C	Time, h	Yield,[a] %
1	$[Rh(C_2H_4)_2Cl]_2$	H-$SiEt_3$	3.0	60	2	88 (86)[b]
2[c]	$RhCl(PPh_3)_3$	H-$SiEt_3$	3.0	60	2	0
3	$[Rh(C_2H_4)_2Cl]_2$	H-Si^iPr_3	3.0	60	2	trace
4	$[Rh(C_2H_4)_2Cl]_2$	H-$SiEt_3$	2.0	60	2	46
5	$[Rh(C_2H_4)_2Cl]_2$	H-$SiEt_3$	4.0	60	2	81
6	$[Rh(C_2H_4)_2Cl]_2$	H-$SiEt_3$	3.0	40	2	75
7	$[Rh(C_2H_4)_2Cl]_2$	H-$SiEt_3$	3.0	80	2	trace
8	$[Rh(C_2H_4)_2Cl]_2$	H-$SiEt_3$	3.0	60	1	58
9	$[Rh(C_2H_4)_2Cl]_2$	H-$SiEt_3$	3.0	60	3	74
10	$[Rh(C_2H_4)_2Cl]_2$	H-$SiEt_3$	3.0	60	4	68

[a]NMR yield: The internal standard is 1,3,5-trimethoxybenzene.
[b]Isolated yield.
[c]Without tris-2,4,6-trimethylphenylphosphine.

conversion was observed. Accordingly, we retained the rhodium precatalyst/ligand combination from entry 1 and varied the identity and loading of the silylation reagent, as well as the temperature and duration of the second stage.

Changing the hydrosilane, from triethylsilane to triisopropylsilane (entry 3) produced only trace amounts of product. Varying the equivalents of triethylsilane (entries 4 and 5) showed that 3.0 equivalents gave the highest yield of **2a**; thus, the conditions in entry 1 were adopted as optimal. Adjusting the temperature (entries 6 and 7) and reaction time (entries 8–10) during the second stage did not improve the outcome, confirming entry 1 as the standard set of conditions for further studies.

2.2 | Substrate Scope

2.2.1 | Substrate Scope 1 (Alkene Groups)

With the optimized conditions in hand, we next investigated substrate scope (Figure 2) to evaluate the influence of alkyl-chain length and substituent class. For substrates bearing a terminal alkene in the alkenyl enol ether moiety, the C6 chain ($n = 3$, **1a**) provided dihydrobenzofuran **2a** in 86% yield, whereas the C8 ($n = 5$, **1b**) and C9 ($n = 6$, **1c**) analogs gave **2b** and **2c** in moderate yields. Substrates **1d**–**1f** bearing internal alkenes furnished **2d**–**2f** in moderate-to-low yields.

These results indicate that product convergence diminishes as the alkyl-chain length increases. We attribute this trend to the equilibrium nature of long-range isomerization: as the chain becomes longer, the population of alkenes is more widely distributed along the backbone, reducing the fraction capable of undergoing cycloisomerization and thus the overall conversion to the product.

A substrate bearing a phenyl substituent (**1g**) delivered cyclized product **2g** in moderate yield. For ester-containing substrates, the nonconjugated ester **1h** afforded **2h** in moderate yield, whereas the conjugated α,β-unsaturated ester **1i** gave neither the desired product **2i** nor detectable intermediates. This outcome likely reflects the greater thermodynamic stability and electron deficiency of α,β-unsaturated esters, which reduces reactivity.

Substrates containing nitrogen-based functionalities (**1j**, **1k**) produced the corresponding products **2j** and **2k** in low yields.

2.2.2 | Substrate Scope 2 (Aryl Groups)

We next examined substituent effects on the benzene ring (Figure 3). With a methoxy group at C3 (**1l**), the corresponding dihydrobenzofuran **2o** was obtained in moderate yield. Substrates **1m**–**1p** bearing *para* substituents revealed that electron-withdrawing groups such as fluoro, chloro, and methoxycarbonyl led to low to moderate yields of **2m**–**2p**, with particularly strong decreases for the fluoro and methoxycarbonyl derivatives. Similar trends were observed for fluoro- and chloro-substituted substrates at C5 (**1q**, **1r**).

Overall, electron-withdrawing substituents reduced product convergence, probably because decreased electron density on the arene attenuates the reactivity of the alkene during the cycloisomerization step.

2.2.3 | Substrate Scope 3 (Silyl Groups)

We also evaluated various silylation reagents (Figure 4). In our prior hydroboration study, the choice of boron reagent

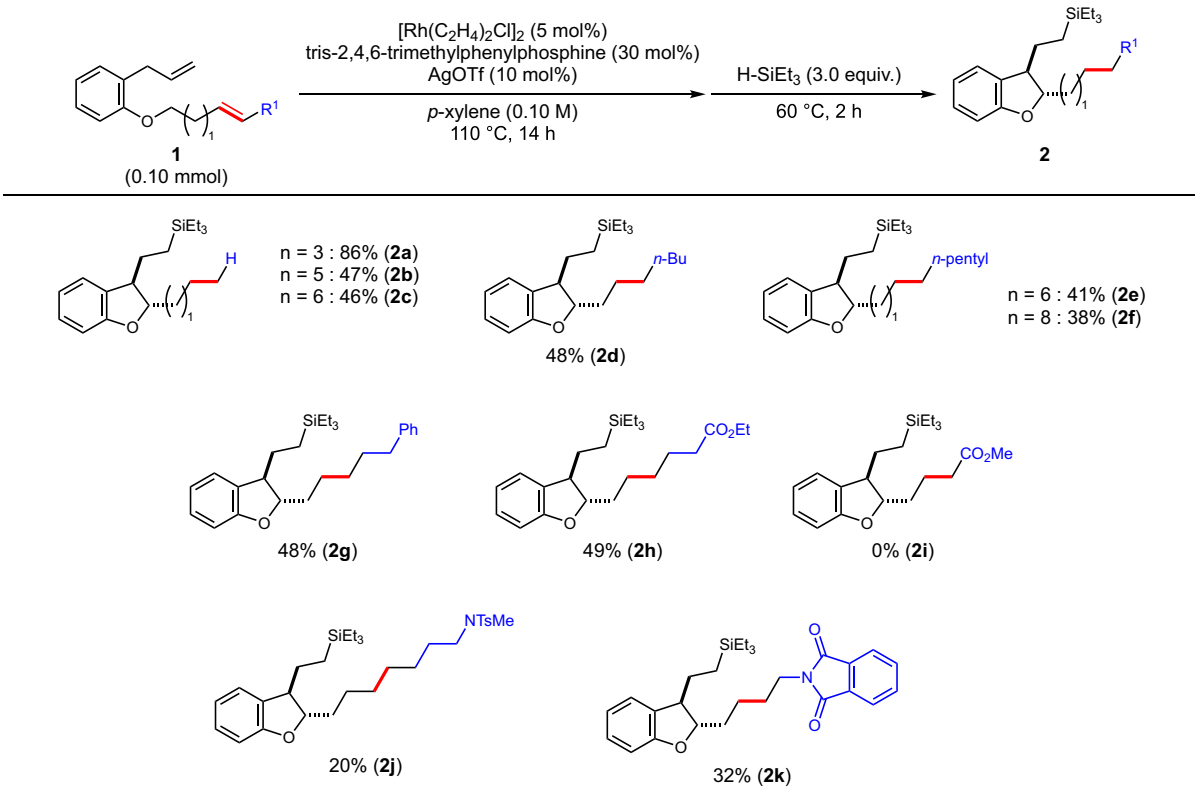

FIGURE 2 | Substrate scope 1 (alkene groups).

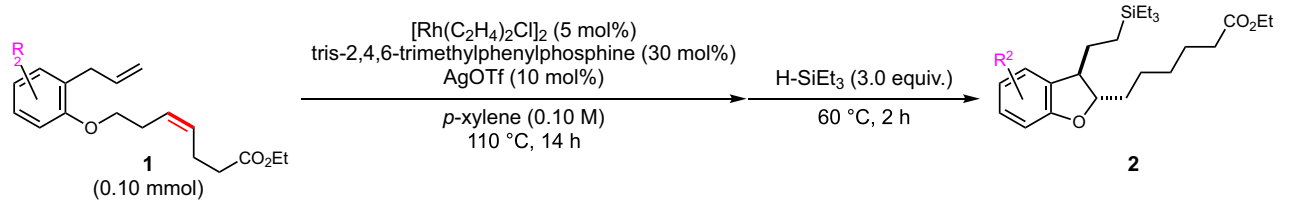

R^2	2	Yield (%)
OMe	**2l**	30

R^2	2	Yield (%)
F	**2q**	17
Cl	**2r**	41

R^2	2	Yield (%)
F	**2m**	26
Cl	**2n**	46
OMe	**2o**	30
CO_2Me	**2p**	19

FIGURE 3 | Substrate scope 2 (aryl groups).

was limited; we therefore explored analogous restrictions in hydrosilylation.

Only a small subset of silylation reagents promoted the reaction in an acceptable yield.

Silyl chlorides, disilanes, and siloxanes were completely ineffective, directing our attention to hydrosilanes. Benzyl-dimethylsilane and dimethylphenylsilane provided the corresponding dihydrobenzofurans **3a** and **3b** in low yields. In contrast, triethoxysilane and triphenylsilane failed to effect hydrosilylation, producing no or only trace product. Several trialkylsilanes were subsequently evaluated, but none were competent. Furthermore, this reaction was performed with secondary silanes. When diethylsilane was

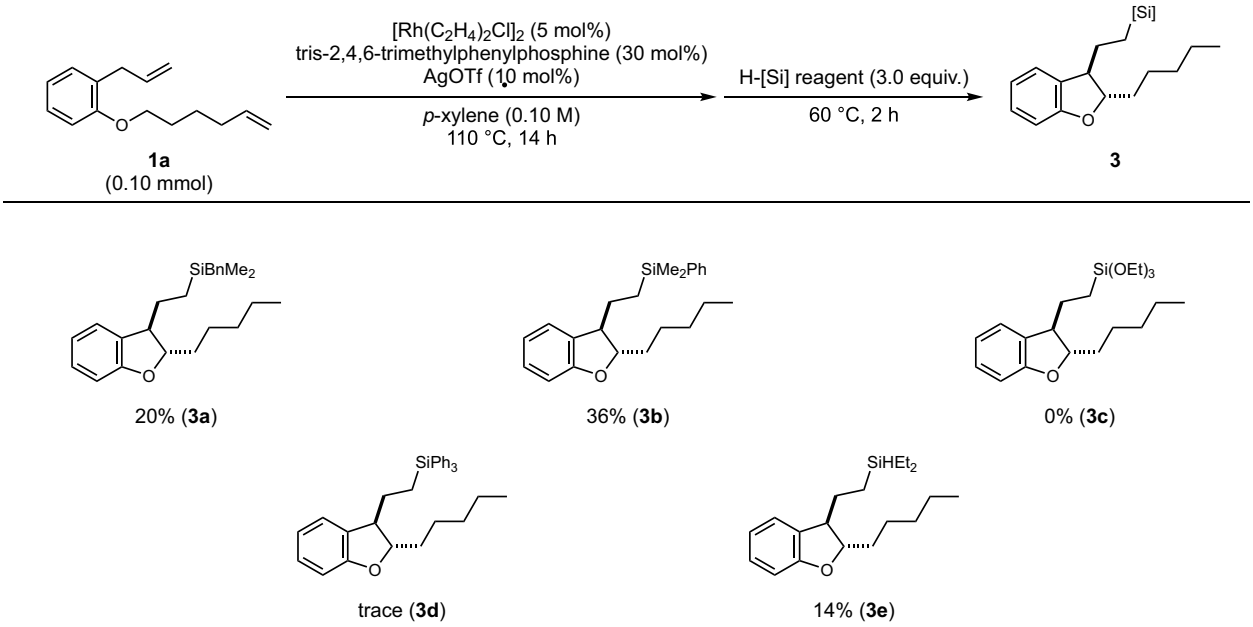

FIGURE 4 | Substrate scope 3 (silyl groups).

used, product **3e** was obtained in 14% yield. Due to the low stability of the product, we did not choose the purification method using the oxidation reaction.

These results indicate that triethoxysilane may induce catalyst deactivation through electronic effect. Moreover, increasing steric congestion around silicon markedly diminishes reactivity, with bulky trialkylsilanes such as triisopropylsilane being particularly ineffective.

2.3 | Gram Scale Experiment

To evaluate scalability, we conducted the reaction on a gram scale (Scheme 1). Using 1.08 g of substrate **1a**, the process proceeded smoothly to provide **2a**, albeit in somewhat reduced yield compared with the small-scale experiment. These results demonstrate that the reaction is not inherently limited by scale and remains effective under preparative conditions.

2.4 | Control Experiments

2.4.1 | Comparison of Reaction Yields

To probe the origin of reactivity differences, we compared outcomes under the conditions of our previous study and the present system (Scheme 2). For a C9 chain substrate, the earlier hydroboration protocol delivered the hydroborated dihydrobenzofuran **4c** in 70% yield, whereas the current hydrosilylation-based conditions afforded the corresponding silylated product **2c** in 46% yield. More generally, the hydrosilylation system provided moderate-to-low yields for most substrates.

2.4.2 | ^{1}H-NMR Experiment

We therefore performed control experiments to identify the cause of the reduced yields relative to hydroboration. Because the sequence involved a two-temperature protocol, we first analyzed the reaction mixture after completion of the first stage by ^{1}H NMR spectroscopy (Figure 5). *p*-xylene-d_{10} was used as the NMR solvent; after quenching the first stage, the solution was transferred from the reaction tube to an NMR tube for measurement. After 14 h, starting material **1a** had been consumed, and signals corresponding to dihydrobenzofuran **4a** and benzofuran **5a** were observed. Additional resonances attributable to unsaturated species appeared at 6.5–5.5 ppm, but no single convergent product dominated. These observations suggest that long-range isomerization, followed by cycloisomerization, yields **4a**, part of which undergoes aromatization to **5a**; species that have not cyclized are also present.

2.4.3 | Comparison With Previous Research

We next examined the divergence from the prior hydroboration system. Under the previous conditions, substrate **1q** underwent long-range isomerization and cycloisomerization to form a

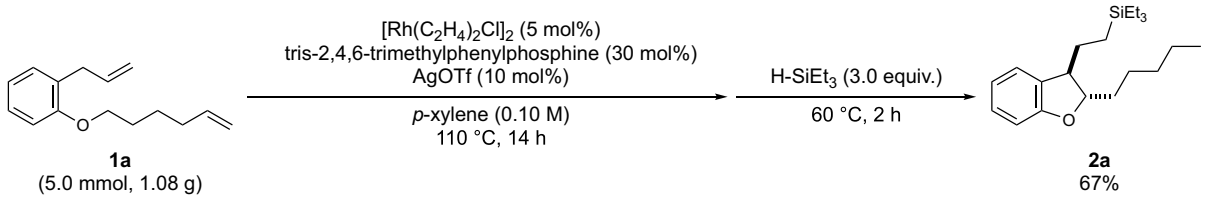

SCHEME 1 | Gram-scale experiment.

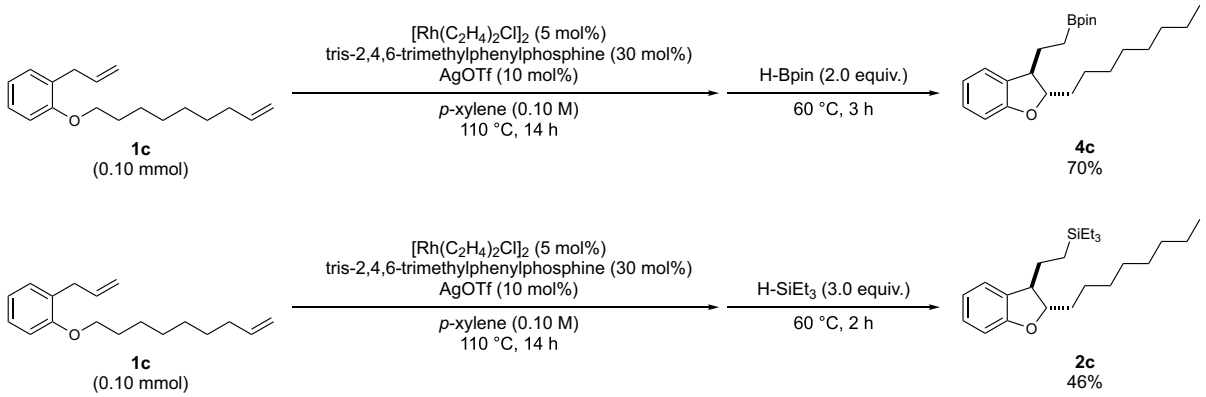

SCHEME 2 | Comparison with some reaction yield.

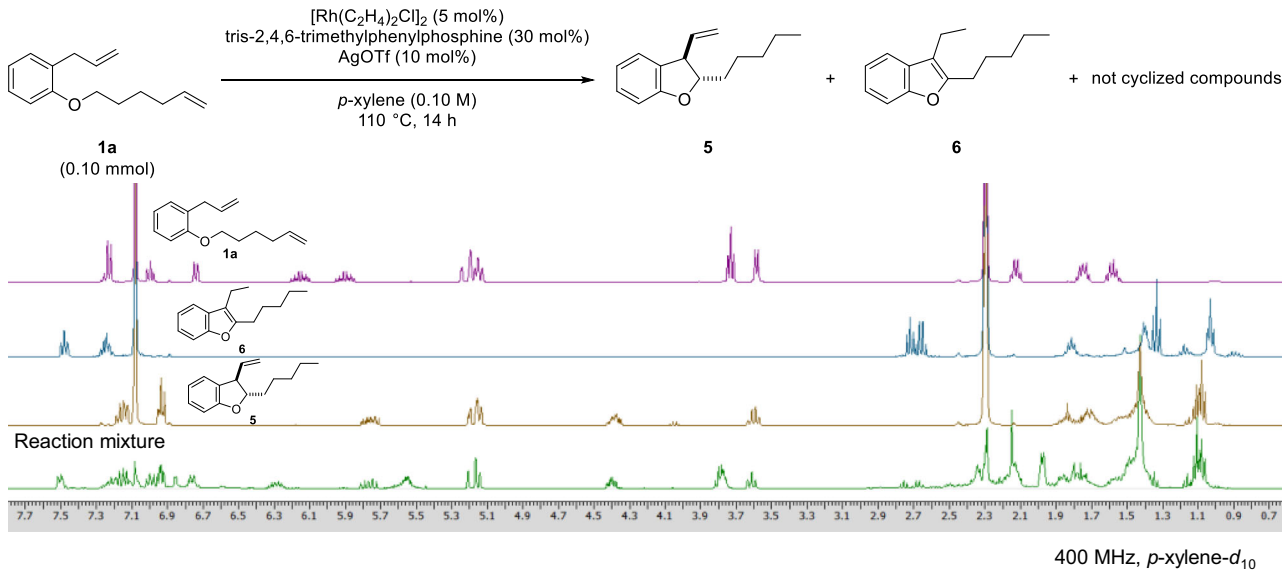

FIGURE 5 | ^{1}H-NMR experiment.

benzofuran core without exception, after which continued isomerization delivered a terminal alkene that underwent selective hydroboration (Scheme 3).

In contrast, in the present hydrosilylation-based system, substrate **1q** afforded only a trace amount of the corresponding product **2q**. Notably, hydrogenated product **7**, derived from the alkene of the postcycloisomerization intermediate, was obtained in 37% yield—an outcome not observed previously. These findings suggest that the functionalization stage generates different active rhodium species depending on the reagent added. With a hydroborane, sufficient rhodium–hydride activity is maintained to sustain long-range isomerization. In the presence of a hydrosilane, however, the concentration of rhodium–hydride species capable of isomerization appears insufficient.

2.5 | Mechanistic Consideration

2.5.1 | Proposed Reaction Pathway

Based on previous reports [23–29], our experimental results, and in situ NMR observations, we propose the mechanism shown in Figure 6. Isomerization of substrate **1** by the rhodium catalyst proceeds without strict preference for either alkene; both double bonds can undergo isomerization. Repeated insertions of rhodium hydride into alkenes and β-hydride eliminations drive chain-walking. Because this process is an equilibrium, it does not inherently converge to a single product. However, when an irreversible downstream event becomes available, the equilibrium can be biased toward that pathway. In the present system, continued isomerization enriches intermediate **G**, from which cycloisomerization forms the benzofuran core, shifting the equilibrium toward cyclization. The resulting intermediate **J** then undergoes rhodium-catalyzed hydrosilylation to furnish silylated dihydrobenzofuran **2**.

2.5.2 | Hypothesis on Nonconvergent Intermediate

The marked yield difference between the current hydrosilylation sequence and the previous hydroboration sequence can be rationalized by considering the distribution of catalytically active species (Figure 7). In the earlier hydroboration system, continued chain-walking after cycloisomerization provides a terminal alkene, which—owing to its higher reactivity relative to internal alkenes—undergoes selective hydroboration to give boron-substituted dihydrobenzofuran **7**. In the present system, by contrast, the catalyst population after cycloisomerization is largely

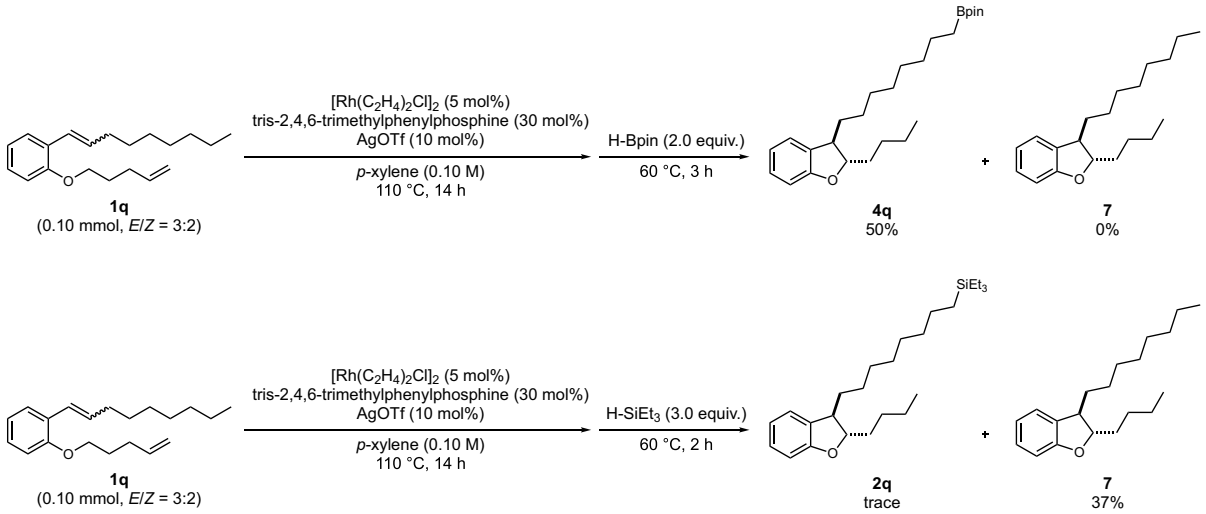

SCHEME 3 | Comparison with previous research.

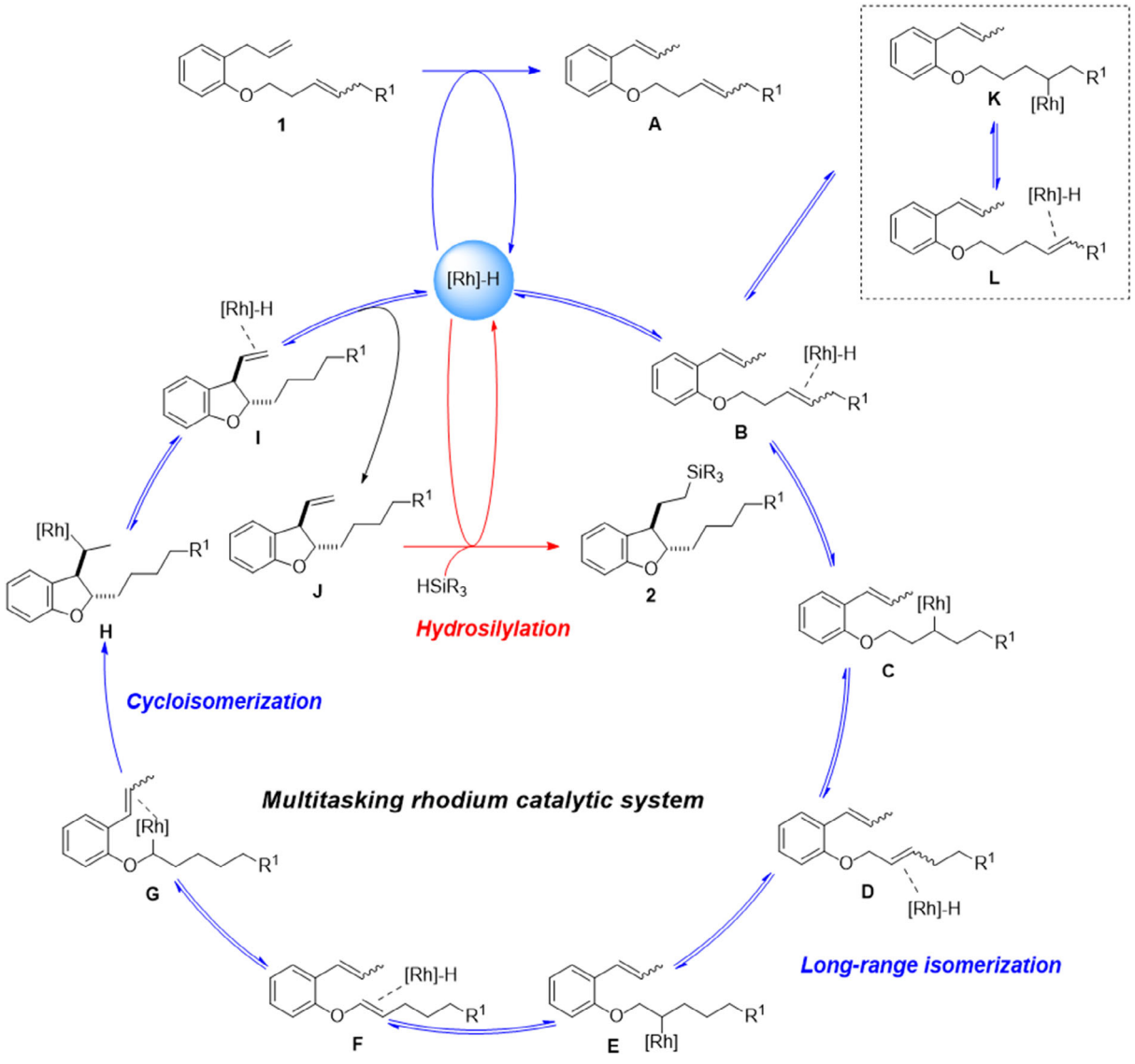

FIGURE 6 | Proposed reaction pathway.

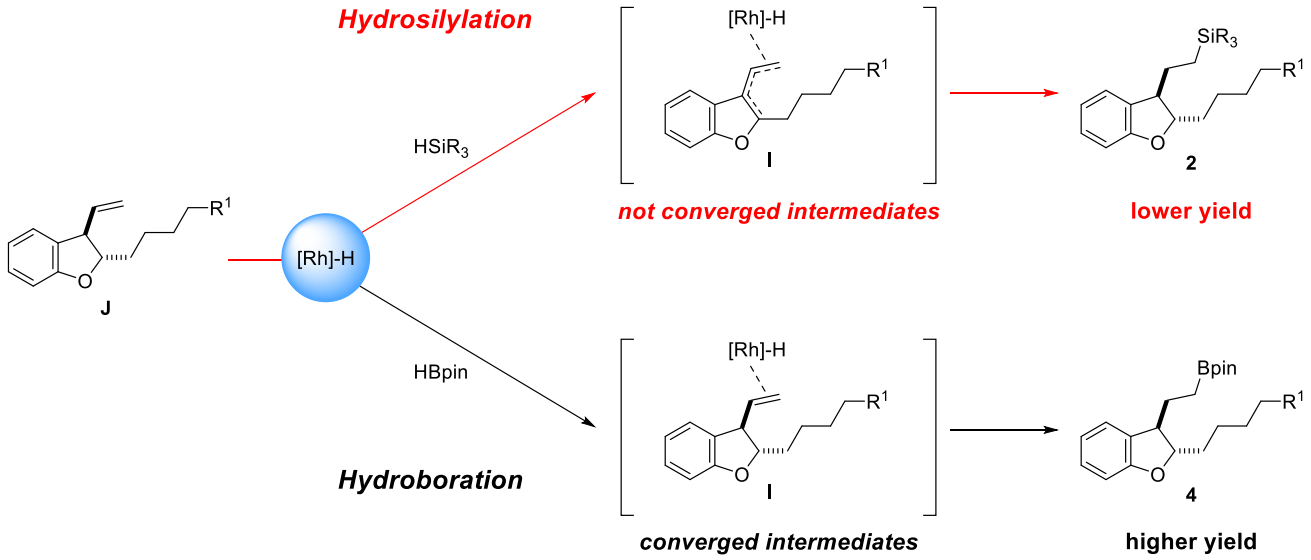

FIGURE 7 | Hypothesis on nonconvergent intermediate.

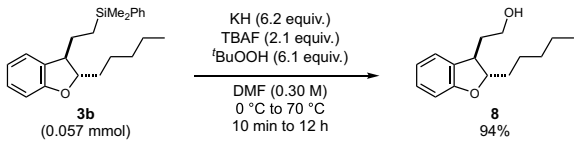

SCHEME 4 | Transformation of the product.

inactive toward further long-range isomerization, preventing convergence to the terminal alkene. Hydrosilylation of the small fraction of terminal alkenes that does exist affords product **2** in comparatively lower yields.

2.6 | Transformation of the Product

Finally, to evaluate the synthetic utility of the products obtained in this reaction, we conducted chemical transformations of the representative product (Scheme 4) [30, 31]. (Transformation reactions of the borylated products have been demonstrated in reference [23]) When the Tamao–Fleming oxidation of dihydrobenzofuran **3b**, bearing a dimethylphenylsilyl group, was examined, the corresponding alcohol **8** was obtained in 94% yield. These results demonstrate that products generated in this reaction are amenable to further chemical transformations.

3 | Conclusion

We have demonstrated a rhodium-catalyzed multitasking sequence comprising long-range isomerization, cycloisomerization, and hydrosilylation. This work extends our previous multitasking rhodium system for one-pot long-range isomerization/cycloisomerization/hydroboration, thereby expanding the repertoire of transformations achievable under a single catalytic framework. More importantly, comparison with the prior system reveals that the functionalization reagent introduced in the final stage profoundly influences the upstream alkene-isomerization equilibrium. In the hydroboration sequence, the added boron reagent promotes continued alkene isomerization and establishes a reaction network that converges on a specific product. In contrast, the addition of a silylation reagent suppresses further isomerization, impeding convergence. These insights are significant for the design of multitasking catalytic systems that orchestrate multiple reactions under a single catalyst, and they provide a conceptual foundation for future advances in this emerging field.

4 | Experimental Section

4.1 | General Procedure for Silylated Dihydrobenzofuran 2

In a glovebox, an oven-dried test tube was added $[Rh(C_2H_4)_2Cl]_2$ (1.94 mg, 5 mol%), tris-2,4,6-trimethylphenylphosphine (11.7 mg, 30 mol%), and anhydrous *p*-xylene (1.0 mL, 0.10 M). The resulting solution was stirred for 30 min at ambient temperature, then AgOTf (2.57 mg, 10 mol%) was added and the reaction mixture was stirred for 30 min.

Next, substrate **1** (0.10 mmol, 1.0 equiv.) was added and the reaction mixture was sealed, removed from the glovebox and heated at 110°C for 14 h. Finally, H-$SiEt_3$ (48 μL, 3.0 equiv.) was added to the reaction mixture and stirred at 60°C for 2 h. After being cooled to room temperature, the reaction mixture was filtered by short silica-gel column chromatography and the filtration was concentrated in vacuo to remove the solvent.

Subsequently, oxidation of the remaining alkenes in the crude mixture with *m*CPBA was conducted to facilitate the isolation of the desired product. The concentrated crude material was dissolved into anhydrous CH_2Cl_2 (0.50 mL, 0.20 M) and *m*CPBA (ca. 65 wt%, 53.1 mg, 2.0 equiv.) were added at 0°C. The resulting mixture was stirred at room temperature for 3 h and subsequently quenched by the addition of a saturated aqueous solution of $Na_2S_2O_3$. The mixture was extracted three times with CH_2Cl_2, and the combined organic portions were washed with brine, dried over Na_2SO_4, filtered, and concentrated. The obtained residue was purified by flash column chromatography on silica gel to give the corresponding 2,3-dihydrobenzofuran **2**.

Author Contributions

Masaharu Takatsuki and **Tsuyoshi Matsuzaki** conducted most of the experiments with guidance from **Yuta Sato**, **Makoto Sako**, **Atsushi Nakayama**, **Takeyuki Suzuki** and **Mitsuhiro Arisawa**. **Masaharu Takatsuki** and **Mitsuhiro Arisawa** drafted the original manuscript. All authors provided input on the manuscript and participated in discussions of the results.

Acknowledgments

This work was supported in parts by the Japan Society for the Promotion of Science (JSPS) KAKENHI (grant number JP23H02608 (M.A.), JST CREST (No. JPMJCR20R1) (M.A.), the Iwatani Naoji Foundation (M.A.), Takahashi Industrial and Economic Research Foundation (M.A.), and the Platform Project for Supporting Drug Discovery and Life Science Research (Basis for Supporting Innovative Drug Discovery and Life Science Research (BINDS)) from AMED under grant number JP25ama121054 (M.A.).

Funding

This work was supported by the Japan Society for the Promotion of Science (JSPS) KAKENHI (Grant JP23H02608), JST CREST (JPMJCR20R1), the Iwatani Naoji Foundation, Takahashi Industrial and Economic Research Foundation, the Platform Project for Supporting Drug Discovery and Life Science Research (Basis for Supporting Innovative Drug Discovery and Life Science Research (BINDS)) from AMED under grant JP25ama121054.

Conflicts of Interest

The authors declare no conflicts of interest.

Data Availability Statement

The data that supports the findings of this study are available in the supplementary material of this article.

References

1. E. Kabir and M. Uzzaman, "A Review on Biological and Medicinal Impact of Heterocyclic Compounds," *Results in Chemistry* 4 (2022): 100606.

2. Y.-H. Miao, Y.-H. Hu, J. Yang, T. Liu, and J. Sun, X.-J Wang "Natural Source, Bioactivity and Synthesis of Benzofuran Derivatives," *RSC Advances* 9 (2019): 27510–27540.

3. G. Sui, T. Li, B. Zhang, R. Wang, H. Hao, and W. Zhou, "Recent Advances on Synthesis and Biological Activities of Aurones," *Bioorganic & Medicinal Chemistry* 29 (2021): 115895.

4. A. Mushtaq, A. F. Zahoor, S. Ahmad, et al., "A Comprehensive Review on Benzofuran Synthesis Featuring Innovative and Catalytic Strategies," *ACS Omega* 9 (2024): 20728–20752.

5. D. Dwarakanath and S. L. Gaonkar, "Advances in Synthetic Strategies and Medicinal Importance of Benzofurans: A Review," *Asian Journal of Organic Chemistry* 11 (2022): e202200282.

6. A. Mushtaq, A. F. Zahoor, S. Ahmad, et al., "A Comprehensive Review on Benzofuran Synthesis Featuring Innovative and Catalytic Strategies," *ACS Omega* 9 (2024): 20728–20752.

7. L. Chiummiento, R. D'Orsi, M. Funicello, and P. Lupattelli, "Last Decade of Unconventional Methodologies for the Synthesis of Substituted Benzofurans," *Molecules*25 (2020): 2327.

8. G. Szőllősi, "Asymmetric One-Pot Reactions Using Heterogeneous Chemical Catalysis: Recent Steps towards Sustainable Processes," *Catalysis Science & Technology* 8 (2018): 389–422.

9. N. T. Patil, V. S. Shinde, and B. Gajula, "A One-Pot Catalysis: The Strategic Classification with Some Recent Examples," *Organic & Biomolecular Chemistry* 10 (2012): 211–224.

10. A. Brodzka, D. Koszelewski, and R. Ostaszewski, "Dual Activity of Grubbs-Type Catalyst in the Transvinylation of Carboxylic Acids and Ring-Closing Metathesis Reactions," *The Journal of Organic Chemistry* 85 (2020): 15305–15313.

11. F.-X. Felpin, J. Coste, C. Zakri, and E. Fouquet, "Preparation of 2-Quinolones by Sequential Heck Reduction–Cyclization (HRC) Reactions by Using a Multitask Palladium Catalyst," *Chemistry–A European Journal* 15 (2009): 7238–7245.

12. F.-X. Felpin and E. Fouquet, "Heterogeneous Multifunctional Catalysts for Tandem Processes: An Approach toward Sustainability," *ChemSusChem* 1 (2008): 718–724.

13. T. Fukuyama and S. Omura, "Multi-Task Catalyst: Ruthenium Hydride Catalyzed Atom-Economical Bond Forming Reactions," *Journal of Synthetic Organic Chemistry Japan* 68 (2010): 649–658.

14. S. Patra and N. Maity, "Recent Advances in (hetero) Dimetallic Systems towards Tandem Catalysis," *Coordination Chemistry Reviews* 434 (2021): 213803.

15. G. K. Zieliński, J. Majtczak, M. Gutowski, and K. Grela, "A Selective and Functional Group-Tolerant Ruthenium-Catalyzed Olefin Metathesis/Transfer Hydrogenation Tandem Sequence Using Formic Acid as Hydrogen Source," *The Journal of Organic Chemistry* 83 (2018): 2542–2553.

16. J. Louie, C. W. Bielawski, and R. H. Grubbs, "Tandem Catalysis: The Sequential Mediation of Olefin Metathesis, Hydrogenation, and Hydrogen Transfer with Single-Component Ru Complexes," *Journal of the American Chemical Society* 123 (2001): 11312–11313.

17. F. Li, L. Lu, and P. Liu, "Acceptorless Dehydrogenative Coupling of o-Aminobenzamides with the Activation of Methanol as a C1 Source for the Construction of Quinazolinones," *Organic Letters* 18 (2016): 2580–2583.

18. Y. Terada, M. Arisawa, and A. Nishida, "Cycloisomerization Promoted by the Combination of a Ruthenium–Carbene Catalyst and Trimethylsilyl Vinyl Ether, and Its Application in the Synthesis of Heterocyclic Compounds: 3-Methylene-2,3-Dihydroindoles and 3-Methylene-2,3-Dihydrobenzofurans," *Angewandte Chemie International Edition* 43 (2004): 4063–4067.

19. J. Qiu, M. Sako, T. Tanaka, et al., "Iridium-Catalyzed Isomerization/Cycloisomerization/Aromatization of N-Allyl-N-Sulfonyl-o-(λ^1-Silylethynyl) aniline Derivatives to Give Substituted Indole Derivatives," *Organic Letters* 23 (2021): 4284–4288.

20. Y. Sato, T. Matsuzaki, T. Takehara, M. Sako, T. Suzuki, and M. Arisawa, "Double Isomerization/Cycloisomerization/Aromatization of 1-(allyloxy)-2-(cyclopropylmethyl)benzenes to Give 2-Ethyl-3-Isopropylbenzofurans Using a Multitasking Single Rhodium Catalyst," *Chemical Communications* 58 (2022): 415–418.

21. R. Grigg, J. F. Malone, T. R. B. Mitchell, A. Ramasubbu, and R. M. Scott, "Palladium- and Rhodium-Catalysed Cyclisation of 1,6-, 1,7- and 1,8-Dienes to Cyclopentenes and Methylene-Cyclopentenes. Crystal Structure of Dichloro(4,4-Diacetylhepta-1,6-Diene)Platinum(II)," *Journal of the Chemical Society, Perkin Transactions 1* 1 (1984): 1745–1754.

22. T. Kochi, K. Ichinose, M. Shigekane, T. Hamasaki, and F. Kakiuchi, "Metal-Catalyzed Sequential Formation of Distant Bonds in Organic Molecules: Palladium-Catalyzed Hydrosilylation/Cyclization of 1,n-Dienes by Chain Walking," *Angewandte Chemie International Edition* 58 (2019): 5261–5265.

23. Y. Sato, M. Nagafuchi, M. Takatsuki, et al., "Multitasking Rhodium-Catalyzed Remote C(sp^3)–H Functionalization Reactions of Acyclic Dienes to Yield Benzene-Fused Heterocycles," *Green Chemistry* 27 (2025): 248–255.

24. R.-Z. Huang, K. K. Lau, Z. Li, T.-L. Liu, and Y. Zhao, "Rhodium-Catalyzed Enantioconvergent Isomerization of Homoallylic and

Bishomoallylic Secondary Alcohols," *Journal of the American Chemical Society* 140 (2018): 14647–14654.

25. N. Wagner-Carlberg and T. Rovis, "Rhodium(III)-Catalyzed Remote Hydroamidation of Internal Alkenes Via Chain Walking," *ACS Catalysis* 13 (2023): 16337–16343.

26. W. Ouyang, J. Rao, Y. Li, et al., "Recent Achievements in the Rhodium-Catalyzed ConciseConstruction of Medium N-Heterocycles, Azepines and Azocines," *Advanced Synthesis & Catalysis* 362 (2020): 5576–5600.

27. J. D. Neuhaus and M. C. Willis, "Homogeneous Rhodium(I)-Catalysis in De Novo Heterocycle Syntheses," *Organic & Biomolecular Chemistry* 14 (2016): 4986–5000.

28. L. Mirghaffari, S. Hosseininezhad, M. Seydi, A. Ramazani, H. Ahankar, and G. Zhang, "Recent Progress of Platinum and Rhodium Catalysts in Hydrosilylation Reactions," *ChemistrySelect* 10 (2025): e202501079.

29. E. D. Amoateng, E. Fosu, and T. K. Hollis, "Highly Regioselective Anti-Markovnikov Hydrosilylation of Alkenes under Mild Conditions: Application of CCC-NHC Pincer Rh Complexes," *Journal of Organometallic Chemistry* 1031 (2025): 123579.

30. J. H. Smitrovich and K. A. Woerpel, "Oxidation of Sterically Hindered Alkoxysilanes and Phenylsilanes under Basic Conditions," *The Journal of Organic Chemistry* 61 (1996): 6044–6046.

31. T. Seiser and N. Cramer, "Rhodium(I)-Catalyzed 1,4-Silicon Shift of Unactivated Silanes from Aryl to Alkyl: Enantioselective Synthesis of Indanol Derivatives," *Angewandte Chemie International Edition* 49 (2010): 10163–10167.

Supporting Information

Additional supporting information can be found online in the Supporting Information section.